PERGAMON

International Journal of Solids and Structures 38 (2001) 3453–3468

INTERNATIONAL JOURNAL OF SOLIDS and STRUCTURES

www.elsevier.com/locate/ijsolstr

A crack near the interface of bonded elastic–viscoelastic planes

X. Han [1], F. Ellyin [*], Z. Xia

Department of Mechanical Engineering, University of Alberta, Edmonton, Alta. T6G 2G8, Canada

Received 18 February 2000; in revised form 16 May 2000

Abstract

The plane problem for bonded elastic–viscoelastic half planes containing an arbitrarily oriented crack in the vicinity of the interface is investigated. By using the Laplace transformation, the viscoelastic problem is first reduced to an associated elastic one. The complex function method is used to solve the associated elastic problem. Then, the solution of viscoelastic problem is obtained by using the inverse Laplace transformation of the associated elastic results. The fracture parameters, such as the stress intensity factors and strain energy release rates, and the probable directions of crack propagation are determined for various crack orientation and distance from the interface. The effect of elastic–viscoelastic interface on a crack approaching it from either medium is discussed.

Keywords: Bonded planes; Near-interface crack; Crack propagation; Energy release rate; Viscoelasticity

1. Introduction

The purpose of this work is to investigate the crack behavior in the vicinity of the interface of bonded elastic–viscoelastic layers. In laminated composite materials, one method to improve the laminate's tolerance to interfacial or through thickness cracks, is to place a thin adhesive layer between certain plies. The adhesive layer is often required to be non-brittle with soft modulus and large failure strain, and is usually a viscoelastic material. In order to estimate the effect of the viscoelastic adhesive layer or the interlay on the fracture behavior, it is necessary to investigate the problem of a crack located near the interface of bonded elastic–viscoelastic media.

The fracture strength of a composite material is controlled, to a considerable extent, by the size, shape, orientation and distribution of flaws and imperfections which exist in the material due to the manufacturing process. If the dominant imperfection is imbedded in a homogeneous phase and is located sufficiently far from the interface, then the stress field around the imperfection will not be affected by the interface. On the other hand, if the flaw is located near a bi-material interface, the effect of interface on the fracture behavior of the nearby crack becomes important. For bonded elastic materials, in additional to the interfacial crack

[*] Corresponding author. Fax: +780-492-2200.
E-mail address: fernand.ellyin@ualberta.ca (F. Ellyin).
[1] Visiting from the Institute of Mechanics, Chinese Academy of Sciences, Beijing 100080 China.

0020-7683/01/$ - see front matter
PII: S0020-7683(00)00225-0

problems, the near interface crack problems have been a subject of active research. They include the special cases of cracks which are parallel or perpendicular to the interface, and the general case of cracks which are oriented arbitrarily with respect to the interface (Cook and Erdogan, 1972; Erdogan and Aksogan, 1974; Lu and Lardner, 1992; Isida and Noguchi, 1993). For bonded elastic–viscoelastic materials, however, only results of anti-plane problems of the interfacial crack and near interface crack are reported in the literature (Sills and Benveniste, 1981, 1983; Atkinson and Chen, 1996; Chang, 1999). For viscoelastic problems, in principle, it may be possible to use the so-called "correspondence principle". The principle enables the linear viscoelastic problems to be reduced to mathematically equivalent elastic ones (the associated elastic problems). With regards to the correspondence principle and viscoelastic problems, the reader is encouraged to consult the literatures, such as works by Lee (1962) and Schapery (1967).

In this paper, the plane problem of an arbitrarily oriented crack located near the interface of bonded elastic–viscoelastic materials is investigated. First, by using the Laplace transform method, the viscoelastic problem is reduced to an associated elastic one. The convenient and powerful complex function method is used to obtain the solution of the associated elastic plane problem. Then, the original viscoelastic solution is obtained by the inverse Laplace transform method. The interface and viscoelastic effects on the fracture parameters (such as stress intensity factors and strain energy release rates) of a near interface crack which approaches the interface from either phase, are investigated through numerical calculations.

2. Constitutive equations of viscoelastic materials

For isotropic linear elastic materials, the stress–strain relation can be expressed in deviatoric form as

$$s_{ij} = 2\mu e_{ij}, \qquad \sigma_{kk} = 3K\varepsilon_{kk}, \tag{1}$$

where s_{ij} and e_{ij} are deviatoric stress and strain tensors, μ and K are shear and bulk moduli, respectively.

For isotropic linear viscoelastic materials, the time dependent stress–strain constitutive equations can be expressed in a differential form as

$$P_1(D)s_{ij} = Q_1(D)e_{ij}, \qquad P_2(D)\sigma_{kk} = Q_2(D)\varepsilon_{kk}, \tag{2}$$

where P_1, Q_1, P_2 and Q_2 represent polynomials of the time derivative operator $D = \partial/\partial t$.

Taking the Laplace transform of Eq. (2), and assuming that prior to time $t = 0$, all stresses and strains are zero, we obtain

$$P_1(p)\hat{s}_{ij}(p) = Q_1(p)\hat{e}_{ij}(p), \qquad P_2(p)\hat{\sigma}_{kk}(p) = Q_2(p)\hat{\varepsilon}_{kk}(p), \tag{3}$$

where the notation $\hat{f}(p)$ denotes the Laplace transform of $f(t)$, i.e.,

$$\hat{f}(p) = L[f(t)] = \int_0^\infty f(t)\exp(-pt)\,\mathrm{d}t.$$

And L^{-1} expresses Laplace inverse transform, i.e., $L^{-1}[\hat{f}(p)] = f(t)$.

By defining the equivalent shear and bulk moduli $\tilde{\mu}$ and $\tilde{K}$, as

$$2\tilde{\mu} = Q_1(p)/P_1(p), \qquad 3\tilde{K} = Q_2(p)/P_2(p), \tag{4}$$

Eq. (3) reduce to the following forms:

$$\hat{s}_{ij}(p) = 2\tilde{\mu}\hat{e}_{ij}(p), \qquad \hat{\sigma}_{kk}(p) = 3\tilde{K}\hat{\varepsilon}_{kk}(p). \tag{5}$$

Comparing Eq. (5) with Eq. (1), it can be seen that the constitutive equations of viscoelastic materials, in the Laplace transformed field, are similar to those of elastic materials. Consequently, a viscoelastic medium

can be treated as an elastic one in the transformed field. The viscoelastic solutions can then be obtained from the associated elastic solutions by using the inverse Laplace transform. In Section 3, we will solve the corresponding elastic problem first, the results of which will hold for viscoelastic materials in Laplace field, with elastic variables and elastic moduli replaced by the corresponding Laplace transformed variables and equivalent moduli.

3. Near-interfacial crack fields

The near-interface crack problem considered is shown in Fig. 1 in which the half planes S_1 and S_2 represent two different materials. The crack is located in one-half plane, without loss of generality, such as in S_2, and the crack geometric parameters are shown in the figure. Quantities in S_1 and S_2 are noted by subscript 1 and 2, respectively. Assuming that the solid is subjected to uniform stresses at infinity, they are denoted as σ_{x1}^{∞} (in S_1), σ_{x2}^{∞} (in S_2), σ_y^{∞} and σ_{xy}^{∞}. The applied stresses in the x direction are related such that to produce constant strains in the x direction at points remote from the crack. The following relation must then hold (Goree and Venezia, 1977; Isida and Noguchi, 1993):

$$\sigma_{x1}^{\infty} = \frac{1}{1+\kappa_1}\left\{\frac{\mu_1}{\mu_2}(1+\kappa_2)\sigma_{x2}^{\infty} + \left[3-\kappa_1 - \frac{\mu_1}{\mu_2}(3-\kappa_2)\sigma_y^{\infty}\right]\right\}, \tag{6}$$

where $\kappa_i = 3 - 4\nu_i$ for plane strain and $\kappa_i = (3-\nu_i)/(1+\nu_i)$ for plane stress, μ_i and ν_i $(i = 1, 2)$ are shear modulus and Poisson's ratio.

Using the superposition technique, the traction-free crack problem in the composite medium under external loads can be expressed as the sum of two parts. The first part is the field for the bonded half planes without any crack and loaded with the external loads. The second part is the disturbed field for the bonded planes having no external loads at infinity but only applied tractions on the crack surfaces which are equal and opposite to the stresses found in the first part solution of the presumed location of the crack. The field of the first part (crack-free) is known. Only the distributed field of the second part needs to be determined, and it is given below.

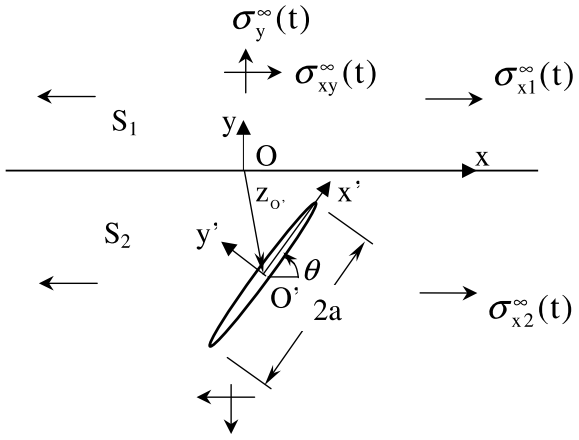

Fig. 1. A crack near the interface of two bonded half planes.

3.1. Formulation of the crack field

For an isotropic elastic body under plane deformation, the stress components can be represented by two complex potentials $\Phi(z)$ and $\Omega(z)$ (Muskhlishvili, 1953; Suo, 1989), as

$$\begin{aligned}\sigma_{xx}+\sigma_{yy}&=2[\Phi(z)+\overline{\Phi(z)}],\\ \sigma_{yy}-\mathrm{i}\sigma_{xy}&=\Phi(z)+\overline{\Omega(z)}+(z-\overline{z})\overline{\Phi'(z)}.\end{aligned}\tag{7}$$

For a single edge dislocation located at $z=s$ in S_2, the complex potentials are given by Suo (1989) as,

$$\Phi(z)=\begin{cases}(1+\Lambda)\Phi_0(z), & z \text{ in } S_1,\\ \Phi_0(z)+\Pi\overline{\Omega_0}(z), & z \text{ in } S_2,\end{cases}\quad \Omega(z)=\begin{cases}(1+\Pi)\Omega_0(z), & z \text{ in } S_1,\\ \Omega_0(z)+\Lambda\overline{\Phi_0}(z), & z \text{ in } S_2,\end{cases}\tag{8}$$

where $\Phi_0(z)=B/(z-s)$, $\Omega_0(z)=\overline{B}/(z-s)+B(\overline{s}-s)/(z-s)^2$, $B=(b_x+\mathrm{i}b_y)\mu_2/\mathrm{i}\pi(\kappa_2+1)$, and

$$\Lambda=\frac{\alpha+\beta}{1-\beta},\qquad \Pi=\frac{\alpha-\beta}{1+\beta},\qquad \alpha=\frac{\mu_1(\kappa_2+1)-\mu_2(\kappa_1+1)}{\mu_1(\kappa_2+1)+\mu_2(\kappa_1+1)},\qquad \beta=\frac{\mu_1(\kappa_2-1)-\mu_2(\kappa_1-1)}{\mu_1(\kappa_2+1)+\mu_2(\kappa_1+1)}.$$

Substituting Eq. (8) into Eq. (7), the field induced by the dislocation can be calculated. In particular, the stress components (in the local coordinate system), along the crack line can be obtained as

$$\sigma_{y'y'}+\mathrm{i}\sigma_{x'y'}=2\overline{B}(s)\mathrm{e}^{2\mathrm{i}\theta}\frac{1}{z-s}+B(s)G_1(z,s)+\overline{B}(s)G_2(z,s),\tag{9}$$

where θ is the angle of the crack line with the interface (Fig. 1), and

$$\begin{aligned}G_1&=\Pi\left[\frac{1}{z-\overline{s}}+\frac{\overline{s}-s}{(\overline{z}-s)^2}-\mathrm{e}^{2\mathrm{i}\theta}\frac{\overline{z}-\overline{s}}{(z-\overline{s})^2}\right],\\ G_2&=\Pi\left[\frac{1}{\overline{z}-s}+\frac{s-\overline{s}}{(z-\overline{s})^2}+\mathrm{e}^{2\mathrm{i}\theta}\frac{(s-\overline{s})(z+\overline{s}-2\overline{z})}{(z-\overline{s})^3}\right]+\Lambda\,\mathrm{e}^{2\mathrm{i}\theta}\frac{1}{z-\overline{s}}.\end{aligned}\tag{10}$$

Changing the right-hand side of Eq. (9) into the local coordinate system $x'O'y'$, it becomes

$$\sigma_{y'y'}+\mathrm{i}\sigma_{x'y'}=2\overline{B}(\xi)\,\mathrm{e}^{\mathrm{i}\theta}\frac{1}{x'-\xi}+B(\xi)G_1(x',\xi)+\overline{B}(\xi)G_2(x',\xi),\tag{11}$$

where x' and ξ are the local coordinates of the points z and s along the crack line, i.e., $z=z_{O'}+x'\mathrm{e}^{\mathrm{i}\theta}$, $s=z_{O'}+\xi\mathrm{e}^{\mathrm{i}\theta}$, with $z_{O'}$ being the coordinate of the point O', and denote $G_i(z,s)=G_i(z_{O'}+x'\mathrm{e}^{\mathrm{i}\theta},z_{O'}+\xi\mathrm{e}^{\mathrm{i}\theta})$ simply by $G_i(x',\xi)$ $(i=1,2)$.

The crack can be modeled by continuously distributed edge dislocations along the crack of length $2a$, with the density function $B(\xi)$ $(|\xi|<a)$ to be determined from the boundary condition of the crack. The stress components along the crack line, due to the continuous distributed dislocations, can be derived through the integration of the effect of a single dislocation field (11) as,

$$\sigma_{y'y'}+\mathrm{i}\sigma_{x'y'}=2\int_{-a}^{a}\overline{B}(\xi)\mathrm{e}^{\mathrm{i}\theta}\frac{1}{x'-\xi}\mathrm{d}\xi+\int_{-a}^{a}[B(\xi)G_1(x',\xi)+\overline{B}(\xi)G_2(x',\xi)]\mathrm{d}\xi.\tag{12}$$

The stress components along the assumed crack line due to external loads are

$$\sigma^0_{y'y'}+\mathrm{i}\sigma^0_{x'y'}=\tfrac{1}{2}(\sigma^\infty_{x2}+\sigma^\infty_{y})(1-\mathrm{e}^{2\mathrm{i}\theta})+(\sigma^\infty_{y}+\mathrm{i}\sigma^\infty_{xy})\mathrm{e}^{2\mathrm{i}\theta}.\tag{13}$$

Thus, the total stress components along the crack surface, would satisfy the traction-free condition, or the disturbed field should have applied tractions on the crack surfaces which are equal and opposite to $\sigma^0_{y'y'}+\mathrm{i}\sigma^0_{x'y'}$, i.e.,

$$2\int_{-a}^{a}\overline{B}(\xi)e^{i\theta}\frac{1}{x'-\xi}d\xi+\int_{-a}^{a}[B(\xi)G_1(x',\xi)+\overline{B}(\xi)G_2(x',\xi)]d\xi=-(\sigma^0_{y'y'}+i\sigma^0_{x'y'}),\quad |x'|<a. \tag{14}$$

This singular integral equation is the governing equation of the crack problem. In addition, the required single value condition of displacement gives the following equation:

$$\int_{-a}^{a}B(\xi)d\xi=0. \tag{15}$$

From the solution of the above governing equation, the dislocation density function $B(\xi)$, and the disturbed crack field are obtained.

3.2. Numerical solution procedure and fracture parameters

The integral equation (14) can be solved numerically by using the Chebyshev polynomial technique (Erdogan et al., 1973), provided the dislocation density function $B(\xi)$ is expressed by the Chebyshev polynomials as

$$B(\xi)=\frac{1}{\sqrt{1-\tau^2}}\sum_{k=0}^{N}a_kT_k(\tau), \tag{16}$$

where $\tau=\xi/a$, $|\xi|<a$, $|\tau|<1$, $T_k(\tau)$ is the Chebyshev polynomial of the first kind, a_k $(k=0,\ldots,N)$ are coefficients to be determined. The Eq. (15) then gives $a_0=0$, and the integral equation (14) takes the form,

$$-2\pi e^{i\theta}\sum_{k=1}^{N}\overline{a}_kU_{k-1}(x'/a)+\sum_{k=1}^{N}a_kg_1(x',k)+\sum_{k=1}^{N}\overline{a}_kg_2(x',k)=-(\sigma^0_{y'y'}+i\sigma^0_{x'y'}),\quad |x'|<a, \tag{17}$$

where $U_k(\ )$ is the Chebyshev polynomial of the second kind, and

$$g_i(x',k)=a\int_{-1}^{1}G_i(x',a\tau)\frac{T_k(\tau)}{\sqrt{1-\tau^2}}d\tau,\quad i=1,2. \tag{18}$$

Eq. (17) with N unknowns a_k $(k=1,\ldots,N)$ can be solved by the simple collocation method, which satisfies the equation at N discrete points x'_i in the interval $|x'|<a$, such as

$$x'_i=a\cos\left(\frac{i\pi}{N+1}\right),\quad i=1,\ldots,N. \tag{19}$$

Furthermore, in the integral calculation of Eq. (18), the Chebyshev numerical integration rule may be used, such that

$$\int_{-1}^{1}\frac{F(\tau)}{\sqrt{1-\tau^2}}d\tau\approx\sum_{j=1}^{N}A_jF(\tau_j),\qquad A_j=\frac{\pi}{N},\qquad \tau_j=\cos\frac{(2j-1)\pi}{2N}. \tag{20}$$

In this manner, the integral in Eq. (18) is reduced into a summation, and Eq. (17) into a system of linear algebraic equations that can be solved easily.

Upon solution of the governing equation, the dislocation density function is known, and the stress and strain at any point of the plane can be obtained. From Eq. (12), the singular stress term at the crack tips along the crack line is

$$\sigma_{y'y'} + \mathrm{i}\sigma_{x'y'} = 2\int_{-a}^{a} \overline{B}(\xi)\mathrm{e}^{\mathrm{i}\theta}\frac{1}{x'-\xi}\mathrm{d}\xi$$
$$= 2\mathrm{e}^{\mathrm{i}\theta}\pi\sum_k \overline{a}_k\left(\eta - \sqrt{\eta^2-1}\right)^k \Big/ \sqrt{\eta^2-1}, \quad \eta = x'/a,\ |\eta| > 1. \tag{21}$$

The stress intensity factor can then be obtained as

$$K = K_{\mathrm{I}} + \mathrm{i}K_{\mathrm{II}} = \lim_{r\to 0}\sqrt{2\pi r}(\sigma_{y'y'} + \mathrm{i}\sigma_{x'y'}) = \sqrt{\pi a}\left[\pm 2\mathrm{e}^{\mathrm{i}\theta}\pi\sum_k (\pm 1)^k \overline{a}_k\right], \tag{22}$$

where r is the distance ahead of the crack tips along the crack line, and the quantities with upper and lower signs refer to the right- and left-hand tips of the crack, respectively. The energy release rate of the crack, in terms of K is given by

$$G = \frac{\kappa_2 + 1}{8\mu_2}|K|^2. \tag{23}$$

When mode II stress intensity factor $K_{\mathrm{II}} \neq 0$, the crack may not propagate along the original crack plane. The probable angle of crack propagation satisfies the relation (Erdogan and Aksogan, 1974),

$$K_{\mathrm{I}}\sin\varphi_{\mathrm{c}} + K_{\mathrm{II}}(3\cos\varphi_{\mathrm{c}} - 1) = 0, \tag{24}$$

where φ_{c} is measured from the crack prolongation line. The energy release rate of the crack propagation along the angle φ_{c} can be determined approximately by

$$G_{\varphi_{\mathrm{c}}} = \frac{\kappa_2 + 1}{8\mu_2}|K'|^2, \tag{25}$$

where $K' = (1/2)\cos(\varphi_{\mathrm{c}}/2)[K_{\mathrm{I}}(1 + \cos\varphi_{\mathrm{c}}) - 3K_{\mathrm{II}}\sin\varphi_{\mathrm{c}}]$.

4. Viscoelastic fields

Upon determining the elastic solution $f = f(C, \sigma)$, where C represents elastic shear and bulk moduli and σ is the external load, the corresponding viscoelastic solution can be obtained by the following procedure. First, replace elastic variables (f and σ) by Laplace transformed variables ($\hat{f}$ and $\hat{\sigma}$), and elastic moduli (C) by the corresponding equivalent moduli ($\tilde{C}$). Then, using the inverse Laplace transform of the associated elastic solution, the viscoelastic solution is obtained, i.e., $f(t) = L^{-1}[\hat{f}(p)]$. We will show the procedure in some details.

In the elastic solution, the coefficients a_k of the Chebyshev polynomials representation are related to material moduli and external loads in addition to geometrical parameters, and can be written as

$$a_k = a_k(\mu_1, K_1, \mu_2, K_2, \sigma_{x2}^{\infty}, \sigma_y^{\infty}, \sigma_{xy}^{\infty}). \tag{26}$$

In the transformed Laplace field, the associated elastic one can be written as

$$\hat{a}_k = \hat{a}_k(\tilde{\mu}_1, \tilde{K}_1, \tilde{\mu}_2, \tilde{K}_2, \hat{\sigma}_{x2}^{\infty}, \hat{\sigma}_y^{\infty}, \hat{\sigma}_{xy}^{\infty}). \tag{27}$$

Note that the equivalent moduli and the transformed external loads in the above formula are all functions of p, thus $\hat{a}_k = \hat{a}_k(p)$. Taking the inverse Laplace transform of $\hat{a}_k$, the viscoelastic solution is obtained, i.e., $a_k(t) = L^{-1}[\hat{a}_k(p)]$.

From Eq. (16), the dislocation density function is

$$B(\xi,t)=\frac{1}{\sqrt{1-\tau^2}}\sum_{k=0}^{N}a_k(t)T_k(\tau). \tag{28}$$

Similarly, from Eq. (22), the stress intensity factor is given by

$$K(t)=\sqrt{\pi a}\left[\pm 2\mathrm{e}^{\mathrm{i}\theta}\pi\sum_{k}(\pm 1)^k\overline{a}_k(t)\right]. \tag{29}$$

For an elastic media, there is a direct relation between the energy release rate and stress intensity factor (Eq. (23)). However, no such relationship exists for a viscoelastic material. The energy release rate for the latter is determined from the integral definition,

$$G=\frac{1}{2\delta}\int_0^{\delta}\overline{\mathbf{t}}(\delta-r)\Delta\mathbf{U}(r)\,\mathrm{d}r,$$

where $\mathbf{t}(r)=\sigma_{y'y'}(r)+\mathrm{i}\sigma_{x'y'}(r)$ are the crack-tip tractions, $\Delta\mathbf{U}(r)=\Delta u_{y'}(r)+\mathrm{i}\Delta u_{x'}(r)$ are the differences of crack-face displacements, and δ is an arbitrary length scale. Through some calculations, finally, the energy release rate of the crack in viscoelastic materials can be determined by

$$G(t)=K(t)L^{-1}\left[\frac{\tilde{\kappa}_2+1}{8\tilde{\mu}_2}\hat{K}(p)\right]. \tag{30}$$

The probable angle of crack propagation may be obtained from

$$K_{\mathrm{I}}(t)\sin\varphi_{\mathrm{c}}(t)+K_{\mathrm{II}}(t)[3\cos\varphi_{\mathrm{c}}(t)-1]=0. \tag{31}$$

The energy release rate of the crack along the angle φ_{c} is then determined by

$$G_{\varphi_{\mathrm{c}}}(t)=[K_{\mathrm{I}}(t)f_1(\varphi_{\mathrm{c}})+K_{\mathrm{II}}(t)f_2(\varphi_{\mathrm{c}})]\left\{L^{-1}\left[\frac{\tilde{\kappa}_2+1}{8\tilde{\mu}_2}\hat{K}_{\mathrm{I}}(p)\right]f_1(\varphi_{\mathrm{c}})+L^{-1}\left[\frac{\tilde{\kappa}_2+1}{8\tilde{\mu}_2}\hat{K}_{\mathrm{II}}(p)\right]f_2(\varphi_{\mathrm{c}})\right\}, \tag{32}$$

where $f_1(\varphi)=(1/2)\cos(\varphi/2)(1+\cos\varphi)$, $f_2(\varphi)=-(3/2)\cos(\varphi/2)\sin\varphi$.

At two special instances, i.e., the initial state $t=0$ and the terminal one $t\to\infty$, the crack fields can be determined simply without Laplace inverse transform, according to the theorem $f(0^+)=\lim_{t\to 0^+}f(t)=\lim_{p\to\infty}p\hat{f}(p)$, $f(\infty)=\lim_{t\to\infty}f(t)=\lim_{p\to 0}p\hat{f}(p)$. Thus, for the material moduli $\tilde{C}$ $(\tilde{\mu},\tilde{\nu},\tilde{E},\tilde{K},\ldots)$, we have $C(0)=\lim_{t\to 0^+}C(t)=\lim_{p\to\infty}\tilde{C}(p)$, $C(\infty)=\lim_{t\to\infty}C(t)=\lim_{p\to 0}\tilde{C}(p)$. In fact, the viscoelastic fields at the two special states, correspond to two elastic ones in which material moduli $C(0)$ and $C(\infty)$ are used.

5. Numerical technique and results

In the elastic solution, quantities are complex functions. For the convenience of the inverse Laplace transform, complex functions are expressed as real and imaginary parts first, i.e., $g=f_1+\mathrm{i}f_2$. The associated functions are $\hat{g}(p)=\hat{f}_1(p)+\mathrm{i}\hat{f}_2(p)$ (where p is a complex quantity also). For the viscoelastic solution, $g(t)=L^{-1}[\hat{f}_1(p)]+\mathrm{i}L^{-1}[\hat{f}_2(p)]$. In the following, the inverse Laplace transform is taken to the function $\hat{f}_1(p)$ and $\hat{f}_2(p)$, not to $\hat{g}(p)$ directly.

To perform the inverse Laplace transform, usually it is not convenient to apply the complex inverse integral directly,

$$f(t) = L^{-1}[\hat{f}(p)] = \frac{1}{2\pi \mathrm{i}} \int_{\gamma-\mathrm{i}\infty}^{\gamma+\mathrm{i}\infty} \hat{f}(p)\mathrm{e}^{pt}\,\mathrm{d}p. \tag{33}$$

Instead, using $p = \gamma + \mathrm{i}y$, and writing $\hat{f}(x + \mathrm{i}y) = u(x,y) + \mathrm{i}v(x,y)$, then the complex inverse integration becomes the following infinite integration:

$$L^{-1}[\hat{f}(p)] = \frac{\mathrm{e}^{\gamma t}}{\pi} \int_0^{\infty} [u(\gamma,y)\cos yt - v(\gamma,y)\sin yt]\mathrm{d}y. \tag{34}$$

There are certain techniques for the evaluation of infinite integral. To keep high convergent speed and accuracy to a slow decay integrand, it is preferable to evaluate the integral in closed form for large argument value. In the problem under consideration, when the external load is a step function $\sigma^{\infty}(t) = \sigma_0^{\infty}H(t)$ (where $H(t)$ denotes the Heaviside unit step function), in the Laplace field, usually $\hat{\sigma}^{\infty}(p) \propto 1/p$, and the associated solution has the form of $\hat{f}(p) = F(p)/p$ with an asymptotic value $F(\infty)/(\mathrm{i}y)$ as $p \to \gamma + \mathrm{i}\infty$. After analyzing the asymptotic behavior, the inverse transform can be calculated by

$$f(t) \approx \frac{\mathrm{e}^{\gamma t}}{\pi}\left\{ \int_0^A [u(\gamma,y)\cos(yt) - v(\gamma,y)\sin(yt)]\mathrm{d}y + F(\infty)\int_A^{\infty} \frac{\sin(yt)}{y}\mathrm{d}y \right\}, \tag{35}$$

where A is a large number. The first integral in Eq. (35) is a finite one, which can be evaluated numerically. The second integral can be obtained in a closed form as

$$\int_A^{\infty} \frac{\sin(yt)}{y}\mathrm{d}y = -\mathrm{si}(tA), \tag{36}$$

where $\mathrm{si}(x) = -\int_x^{\infty}(\sin t/t)\mathrm{d}t$ is the known sine integral. The proper selection of the large number A requires trial calculation. A similar technique for the inverse Laplace transform has been used by Delale and Erdogan (1981). When A is quite large, the numerical result becomes insensitive to it. In fact, we can select a large enough A which satisfies the condition $\mathrm{si}(tA) = 0$, then the second integral in Eq. (35) is zero, and only the regular finite integral needs to be calculated. In this problem, we select $tA = 629.8909$ (when t is not large, such as $t < 10$, however, for larger values of t, a larger tA can be selected, if necessary), which satisfies $\mathrm{si}(tA) = 0$, and yields accurate enough results. The numerical results are also insensitive to the choice of constant γ. In the problem under consideration, for $\hat{f}(p)$, no singularities lie in the right-hand plane $\mathrm{Re}(p) > 0$. So γ can be any positive constant.

In the numerical calculation, a combination of a viscoelastic and elastic materials is used as an example. It is assumed that material 1 is a viscoelastic one, e.g., epoxy polymer with the following properties at the initial time $t = 0$:

$$E_0 = 3.4\ \mathrm{GPa}, \quad \nu_0 = 0.3.$$

At the initial time, other material parameters such as the shear and bulk moduli, can be calculated in terms of E_0 and ν_0, e.g., $\mu_0 = E_0/[2(1+\nu_0)]$ and $K_0 = E_0/[3(1-2\nu_0)]$. The viscoelastic behavior of the material is represented by a combination of elastic (springs) and viscos (dashdots) elements. Here, the epoxy shear modulus is modeled by the standard linear solid (Fig. 2). It is assumed $\mu_{\infty} = \mu_0/10$ and the relaxation time of the shear modulus is τ_{G}. The parameters G_1, G_2 and η_2 of the standard linear solid viscoelastic model can be determined from μ_0, μ_{∞} and τ_{G}. For the epoxy polymer, it is also assumed that the bulk modulus K is a constant, i.e., $K = K_0$. Thus, the viscoelastic material model is now completely specified. The parameters and relations of the viscoelastic model are given in the appendix. Fig. 3 shows the material properties, including relaxation moduli (both shear modulus $\mu(t)$ and extension modulus $E(t)$) and shear creep compliance $J(t)$ of the epoxy polymer described above. The normalized time τ, is the retardation time of $J(t)$, which is related to the relaxation time τ_{G} by $\tau = \tau_{\mathrm{G}}\mu_0/\mu_{\infty}$ (see Appendix A).

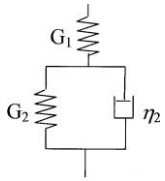

Fig. 2. Standard linear viscoelastic solid model.

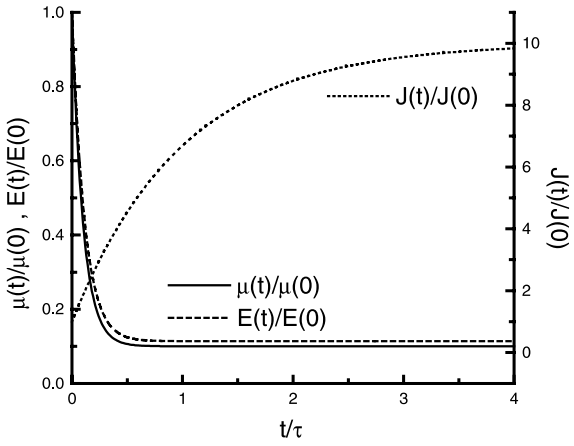

Fig. 3. Viscoelastic material properties, including relaxation moduli and creep compliance.

It is assumed that material 2 is elastic, e.g., glass, with the following elastic constants:

$$E = 85 \text{ GPa}, \quad \nu = 0.2.$$

All of the other moduli of the glass are constant and can be determined accordingly.

The numerical calculation is for the plane strain condition. These results are for the remote uniform loading condition,

$$\sigma_y^{\infty}(t) = \sigma_y^{\infty} H(t), \qquad \sigma_{xy}^{\infty}(t) = \sigma_{xy}^{\infty} H(t), \qquad \varepsilon_x^{\infty}(t) = \varepsilon_x^{\infty} H(t),$$

where $H(t)$ denotes the Heaviside unit step function. For convenience, $\sigma_{x2}^{\infty}(t) = \sigma_{x2}^{\infty} H(t)$ is often used as the external loading in x direction instead of $\varepsilon_x^{\infty}(t)$. The remote stress $\sigma_{x1}^{\infty}(t)$ has a relation with $\sigma_{x2}^{\infty}(t)$ and $\sigma_y^{\infty}(t)$, which satisfies Eq. (6) in the Laplace field. It is also noted that although $\sigma_{x2}^{\infty}(t)$ and $\sigma_y^{\infty}(t)$ are constants, $\sigma_{x1}^{\infty}(t)$ changes with time, because the moduli of the viscoelastic material change with time. This relation is shown in Fig. 4. From the figures, we can see that $\sigma_{x1}^{\infty}(t)$ has a similar trend as the shear modulus $\mu(t)$ of the viscoelastic material. It also has a similar intrinsic characteristic time as that of $\mu(t)$ (the relaxation time τ_G which equals 0.1τ for the assumed material, can be considered as the intrinsic characteristic time of $\mu(t)$). But the trend of $\sigma_{x1}^{\infty}(t)$ is quite different from that of the creep compliance (Fig. 4(a)). The stress $\sigma_{x1}^{\infty}(t)$ is greatly influenced by the stress component $\sigma_y^{\infty}(t)$ in y direction (Fig. 4(b)). The results to follow are for the remote loading which is parallel to the interface, with $\sigma_{x2}^{\infty}(t)$ equals the unit step function $H(t)$ (and $\sigma_{x1}^{\infty}(t)$ is related to $\sigma_{x2}^{\infty}(t)$). The stress intensity factors (SIF) are normalized (divided) by $\sqrt{\pi a}$; the strain energy release rates are normalized by $G_0 = (\kappa_2 + 1/8\mu_2)\pi a$, which is the corresponding value for a crack in material 2, far away from the interface and normal to the loading direction.

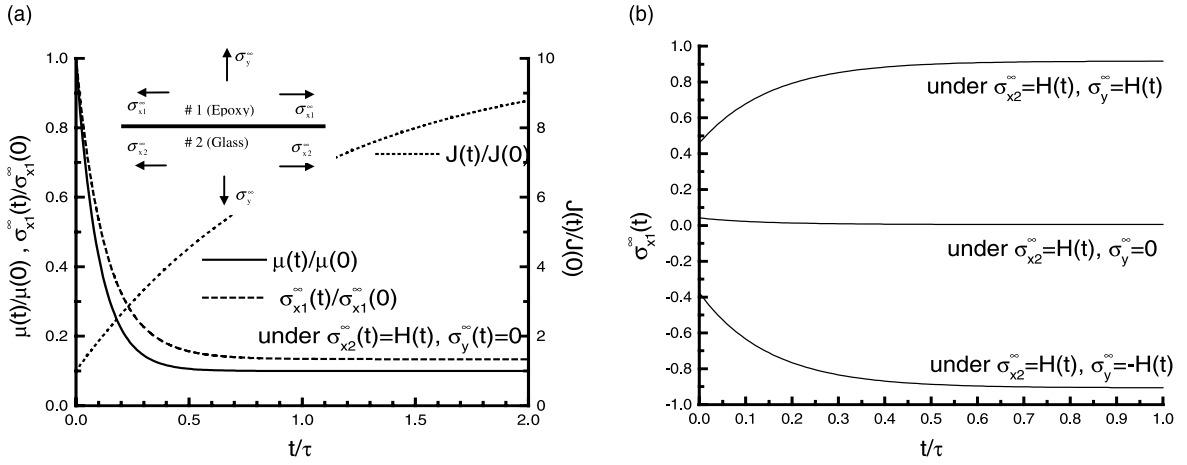

Fig. 4. (a) The variation of stress component $\sigma_{x1}^{\infty}(t)$ with time under applied loading $\sigma_{x2}^{\infty} = H(t)$ and $\sigma_{y}^{\infty} = 0$. (b) The variation of stress component $\sigma_{x1}^{\infty}(t)$ with time under applied loading $\sigma_{x2}^{\infty} = H(t)$ and different σ_{y}^{∞} values.

To check the accuracy of the present method, the results for a crack near the interface of bonded elastic half planes, are compared with those of Erdogan and Aksogan (1974) and Isida and Noguchi (1993), at the limit cases $t = 0$ or $t \to \infty$. The agreement is indeed very good. The values of stress intensity factors agree up to third or fourth digit. The present method yields results with high accuracy and fast convergence rate, provided the crack tip is not too close to the interface. As the crack tip approaches the interface, more polynomial terms for the dislocation density (and corresponding collocation points) are required. For example, to keep the stress intensity factors within 4 digits accuracy, about 20–30 terms are needed, if the distance of crack tip to interface $h/a = 0.1$. For a crack not normal to the interface, especially when about parallel to the interface, usually more terms are needed when h/a is quite small. For example, for a normal crack with $h/a = 0.01$, about 60 terms are sufficient, while for a parallel crack with $h/a = 0.02$, more than hundred terms are necessary.

Figs. 5–8 show the effects of interface and viscoelasticity on fracture parameters of a crack near the interface, under remote loading parallel to the interface. The effect of interface when the crack is under pressure on its surfaces, is depicted in Figs. 9 and 10.

6. Discussion of results

Under remote uniform loading parallel to the interface, the variation of the stress intensity factors K (mode I) and strain energy release rates G at crack tips, are shown in Fig. 5 as the crack approaches the interface at a right angle from material 2 (the stiffer material, e.g. glass). In contrast, Fig. 6 depicts the same fracture parameters as the crack approaches the interface from material 1 (the softer viscoelastic material, e.g. epoxy). It is seen from Fig. 5 that K and G increase rapidly as the crack approaches the interface from the stiffer material 2, and the values at near tip A increase at a faster rate than those at the far tip B. Conversely, K and G decrease as the crack approaches the interface from softer material 1, and the values at the near tip A decrease at a faster rate than those at the far tip B (Fig. 6(a)). A comparison of Figs. 5 and 6(a) indicates that a crack can easily grow towards an interface from a medium of higher modulus (elastic material) than that of a lower modulus (viscoelastic material). This is a well-known behavior for a crack approaching an interface. It is also seen that when the crack is some distance away from the interface, such

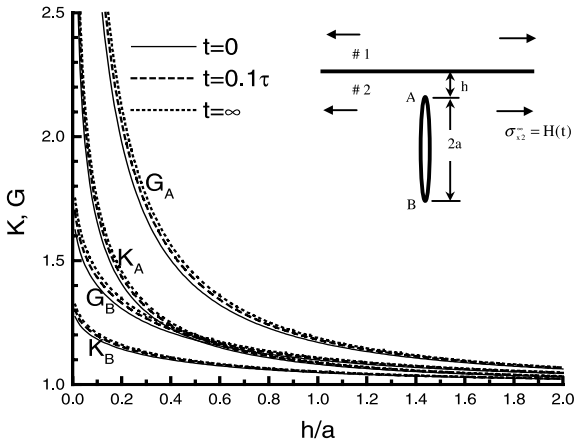

Fig. 5. The trend of stress intensity factors and energy release rates as a crack approaches the interface perpendicularly from the stiffer material 2 (glass), when subjected to uniform loading parallel to the interface.

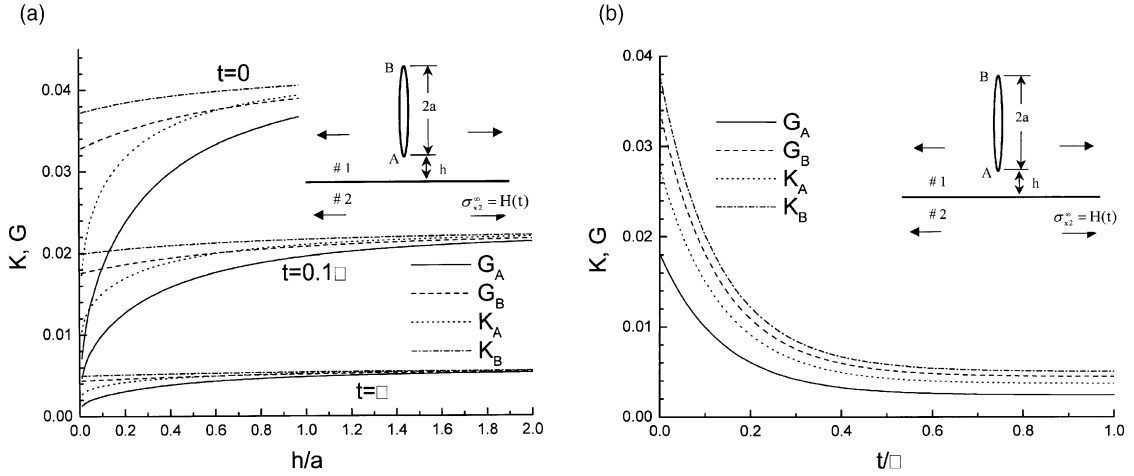

Fig. 6. (a) The trend of stress intensity factors and energy release rates as a crack approaches the interface perpendicularly from the softer material 1 (epoxy), when subjected to uniform loading parallel to the interface. (b) The variation of stress intensity factors and energy release rates with time for a crack in the viscoelastic medium at a distant $h = 0.1a$ from the interface.

as $h > a$, K and G do not vary much, and the influence of interface is quite small. From Fig. 5, it is also seen that K and G only change (here increase) a small amount with time. This indicates that the crack field in the elastic medium is nearly unaffected by the viscoelastic behavior of the softer adjacent medium. On the other hand, from Fig. 6 it is seen that K and G of the crack in the viscoelastic medium change (here decrease) considerably with time. The variation with time is shown more clearly in Fig. 6(b) for a crack at a distance $h = 0.1a$, and they indicate a similar trend as the stress component $\sigma_{x1}^{\infty}(t)$ in the viscoelastic medium (Fig. 4). When comparing the fracture parameters in Fig 6(a) (crack in the softer material) with those in Fig. 5 (crack in the stiffer material), it can be seen that the corresponding values are much smaller.

For a crack in the elastic medium (material 2) approaching the interface at an angle $\theta = 45°$, the stress intensity factor and the energy release rate are shown in Fig. 7(a) for the near tip A. The same is shown in

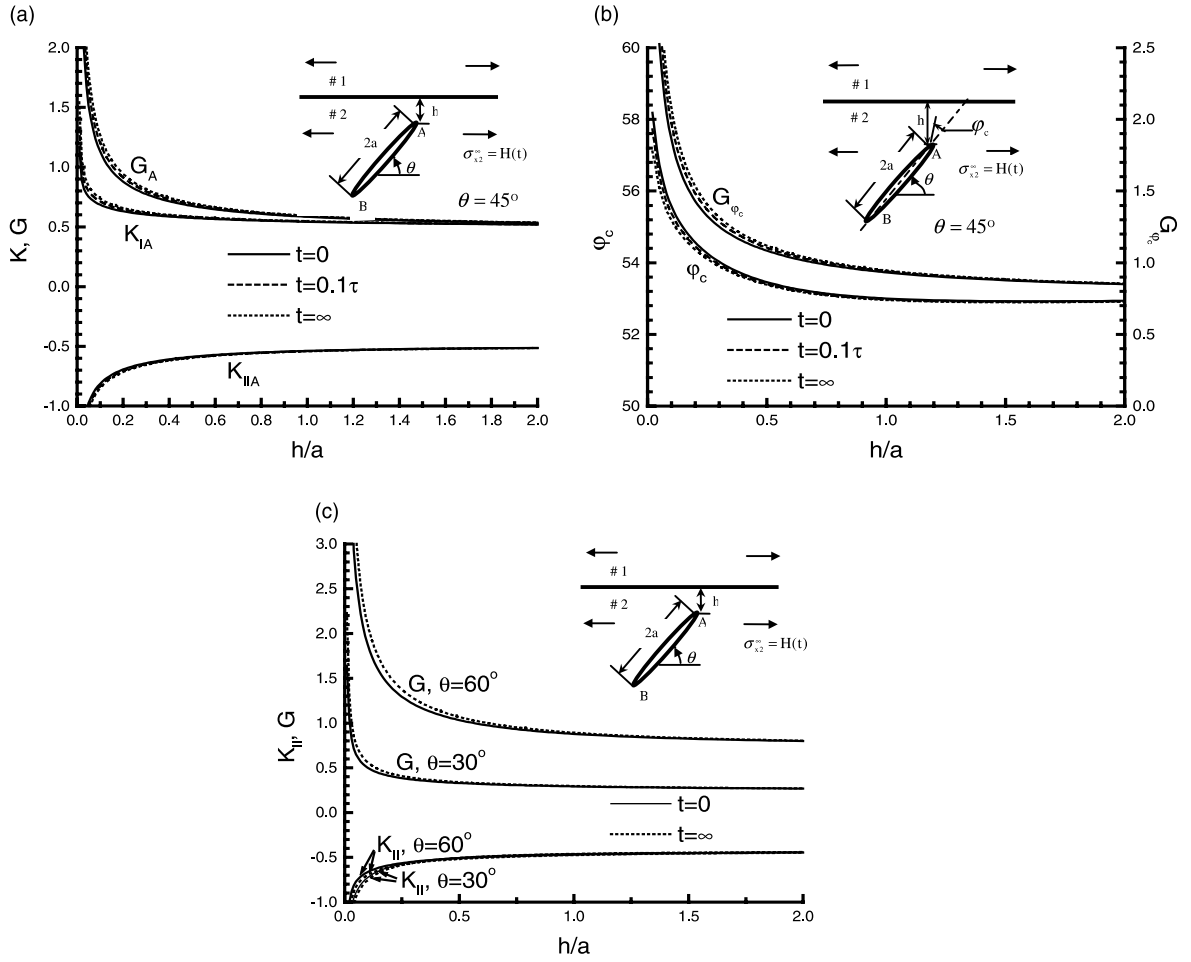

Fig. 7. (a) Stress intensity factors and energy release rate at crack tip A, as the crack approaches the interface with an angle $\theta = 45^\circ$ from material 2 (elastic). (b) Cleavage angle and energy release rate along it at crack tip A, as it approaches the interface with an angle $\theta = 45^\circ$ from material 2. (c) Stress intensity factor K_{II} and energy release rate at crack tip A, as it approaches the interface with different angles from material 2.

Fig. 8(a) for a crack approaching the interface from material 1 (viscoelastic one). It can be seen that the stress intensity factors and energy release rates have similar trends with respect to distance and time as those of normal cracks (compare Figs. 5 and 6(a) with Figs. 7(a) and 8(a)). In contrast to cracks normal to the interface and loading direction, for inclined cracks, in addition to mode I, there is also a mode II stress intensity factor. This implies that an inclined crack ($\theta \neq 90°$) would propagate in a curve path. Figs. 7(b) and 8(b) show the probable cleavage angle φ_c and the energy release rate G_{φ_c} along the angle φ_c at the near interface crack tip A, as the crack with the initial angle $\theta = 45°$ approaches the interface, from materials 2 and 1, respectively. It is seen that all angles φ_c are positive and the direction of crack propagation approximately tends toward normal to the external loading direction, irrespective from which material it approaches the interface. Note, however, that the value of φ_c is different depending on which medium the crack is located. For cracks with other angles ($\theta = 60°$ and $30°$), K_{II} and G at the near crack tip are shown in Figs. 7(c) and 8(c) for cracks in material 2 and 1, respectively. It can be seen that mode II stress intensity

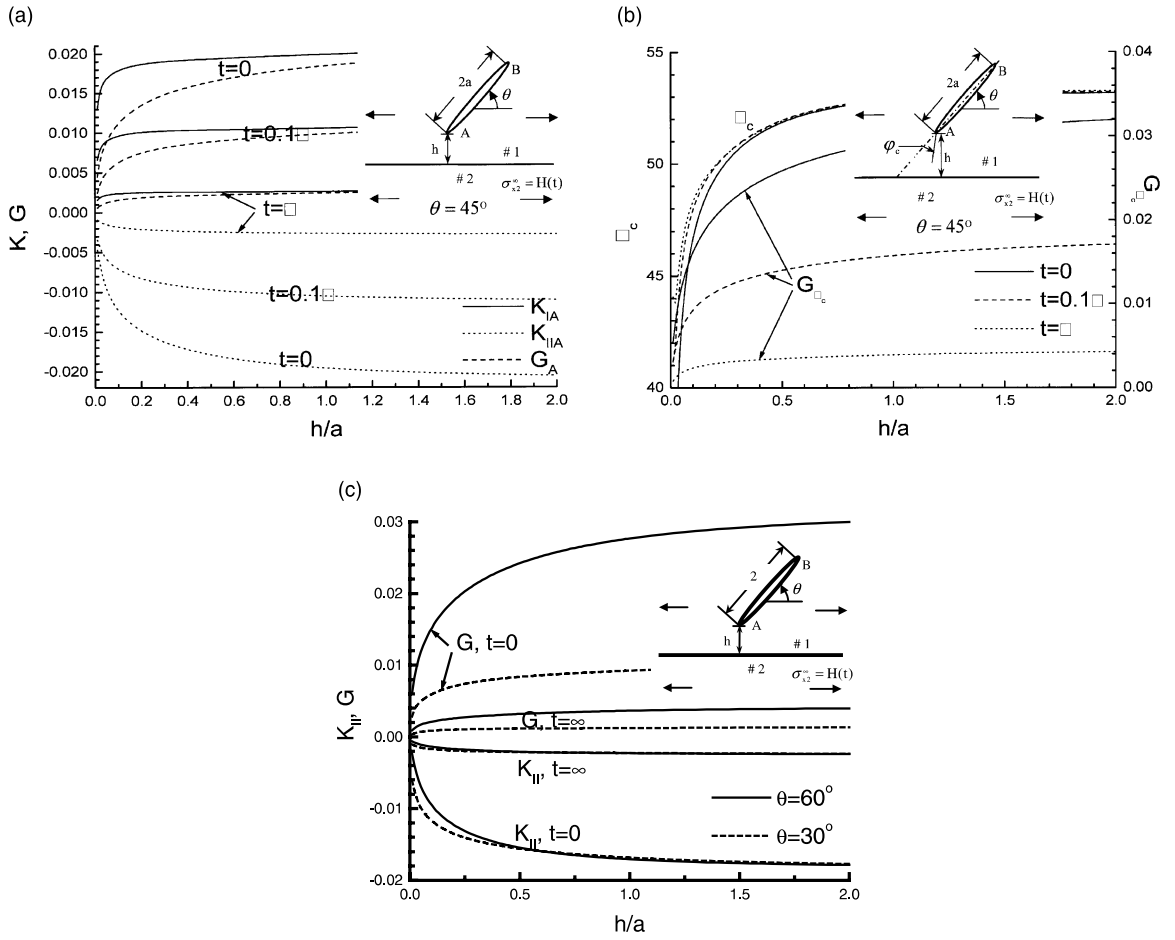

Fig. 8. (a) Stress intensity factors and energy release rate at crack tip A, as the crack approaches the interface with an angle $\theta = 45°$ from material 1 (viscoelastic). (b) Cleavage angle and energy release rate along it at crack tip A, as it approaches the interface with an angle $\theta = 45°$ from material 1. (c) Stress intensity factor K_{II} and energy release rate at crack tip A, as it approaches the interface with different angles from material 1.

factors are always negative, which implies that the crack propagation angles are always positive and tend to propagate perpendicular to the external loading direction. The trend for the crack cleavage direction predicted herein was also indicated by Erdogan and Aksogan (1974) for cracks in bonded elastic materials under far external loadings.

For a crack subjected to a uniform normal pressure $H(t)$ on its surfaces, the values of G and K_{II} at the near crack tip A, as the crack approaches the interface from material 2 and material 1 are shown in Figs. 9 and 10, respectively. Similar to the case of remote loading condition, G increases as the crack approaches the interface from the stiffer material 2, and decreases, for the softer material 1. The crack field changes slightly with time when the crack is located in the elastic material 2, but time has significant effect (the crack field increases significantly with time) on the crack field which is located in the viscoelastic material 1. In contrast to the case of remote loading parallel to the interface, under the normal loading on the crack surfaces (including remote loading normal to the interface), the energy release rate G, for a crack located in the softer material is higher than that of a crack located in the stiffer material. When the crack approaches

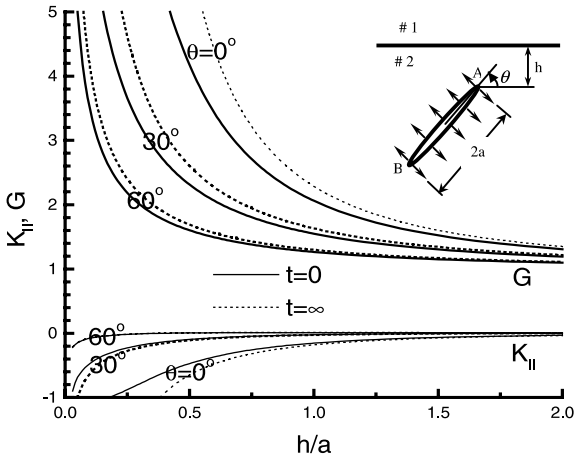

Fig. 9. Stress intensity factor K_{II} and energy release rate at crack tip A, as the crack approaches the interface with different angles from material 2 (elastic), when subjected to uniform pressure $H(t)$ normal to the crack surfaces.

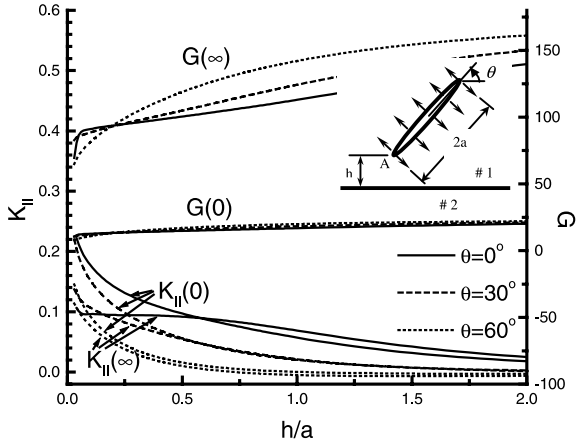

Fig. 10. Stress intensity factor K_{II} and energy release rate at crack tip A, as the crack approaches the interface with different angles from material 1 (viscoelastic), when subjected to uniform pressure $H(t)$ normal to the crack surfaces.

the interface from the medium with a higher modulus, K_{II} become negative (Fig. 9), which indicates that the crack tends to propagate towards the interface. Correspondingly, when the crack approaches the interface from the medium with a lower modulus, the positive K_{II} (as shown in Fig. 10) indicates that the crack tends to propagate away from the interface. With regard to the propagation trend of near-interface cracks which are loaded normal to the crack surfaces, similar results have been reported by He and Hutchinson (1989), and Lu and Lardner (1992) for elastic materials.

7. Conclusions

In this paper, the plane problem of bonded elastic–viscoelastic half planes containing an arbitrarily oriented crack near the interface is considered. The viscoelastic problem is reduced to an associated elastic

one by using the Laplace transform. After solving the associated elastic problem by the method of complex potential functions, the original viscoelastic solution is obtained by taking the inverse Laplace transform to the associated elastic result. As an illustrative example, a crack near the interface of bonded materials, glass (elastic one) and epoxy (viscoelastic one) is considered. The fracture parameters of the crack located in either the stiffer elastic material or the softer viscoelastic material, are analyzed. The interface and time effects on the crack fields are investigated. The results indicate the following trends.

Under constant external loadings, the crack fields do not change significantly with time when the crack is located in the elastic material. On the other hand, when the crack is located in the viscoelastic material, the stress fields, stress intensity factor and energy release rate of the crack vary significantly with time. The variation with time follows a similar trend as the moduli of the viscoelastic material.

When the crack approaches the interface from the stiffer material, the fracture parameters increase, and this indicates that the crack is likely to propagate towards the adjacent softer material. Conversely, as the crack approaches the stiffer material, the fracture parameters decrease, which imply that the adjacent stiffer material will prevent the crack from propagating towards the interface. When a finite crack is a certain distance away from the interface, about a distance of one half of crack length (from the near-crack tip to the interface), the influence of the interface is quite small.

Under a remote loading parallel to the interface, the energy release rate of a crack located in the softer material is smaller than that of a crack in the stiffer material. Through the analysis of crack propagation angles, it is shown that cracks tend to propagate perpendicular to the external loading direction under the parallel loading to the interface.

When a crack is loaded normal to its surfaces, the energy release rate of a crack located in the softer material is larger than that of a crack in the stiffer material (under the same surface loading). This is different from the case of a crack under the external loading parallel to the interface. Under this surface loading, when the crack approaches the interface with a softer adjacent material, the crack will tend to propagate toward the interface. In contrast, the crack will tend to propagate away from the interface when it approaches the interface with a stiffer adjacent medium. For a crack near and about parallel to the interface, when the applied far field load is normal to the interface, the same type of crack propagation trends are observed.

Acknowledgements

This investigation is part of a program concerned with the damage development and crack propagation in polymeric composites. The research is supported, in part, by the Natural Sciences and Engineering Research Council of Canada (NSERC), through grants to F.E. and Z.X.

Appendix A

A viscoelastic material described by the standard linear solid shown in Fig. 2, has the stress–strain relation,

$$(a_1 D + 1)s_{ij} = (b_1 D + b_0)e_{ij}, \tag{A.1}$$

with $a_1 = \eta_2/(G_1 + G_2)$, $b_0 = 2G_1G_2/(G_1 + G_2)$, $b_1/b_0 = \eta_2/G_2$, and D is the time derivative operator, $\partial/\partial t$.

The equivalent shear modulus is then given by

$$2\tilde{\mu} = \frac{b_1 p + b_0}{a_1 p + 1}. \tag{A.2}$$

where p signifies the transformed variable in the Laplace operation.

The shear relaxation modulus (shear stress under unit step shear strain) is

$$2\mu(t) = 2G_1\left\{1 - \frac{G_1}{G_1 + G_2}[1 - \exp(-t/\tau_G)]\right\} \tag{A.3}$$

with $\mu_0 = G_1$, $\mu_\infty = G_1G_2/(G_1 + G_2)$, and shear (modulus) relaxation time $\tau_G = \eta_2/(G_1 + G_2)$.

The shear creep compliance (shear strain under a unit step shear stress) is

$$J(t) = L^{-1}\frac{1}{p2\tilde{\mu}} = \frac{1}{2G_1} + \frac{1}{2G_2}[1 - \exp(-t/\tau)] \tag{A.4}$$

with shear (compliance) retardation time $\tau = \eta_2/G_2$, and $\tau = (\mu_0/\mu_\infty)\tau_G$.

The extension relaxation modulus can be obtained from the relation,

$$\tilde{E} = \frac{9\tilde{K}\tilde{\mu}}{3\tilde{K} + \tilde{\mu}}. \tag{A.5}$$

For the case of $K =$ constant,

$$E(t) = E_0 - (E_0 - E_\infty)[1 - \exp(-t/\tau_E)], \tag{A.6}$$

with $E_0 = 9K\mu_0/(3K + \mu_0)$, $E_\infty = 9K\mu_\infty/(3K + \mu_\infty)$ and $\tau_E = (E_\infty/E_0)\tau$.

References

Atkinson, C., Chen, C.Y., 1996. The influence of layer thickness on the stress intensity factor of a crack lying in an elastic (viscoelastic) layer embedded in a different elastic (viscoelastic) medium (mode III analysis). International Journal of Engineering Science 34, 639–658.

Chang, R.C., 1999. Finite thickness cracked layer bonded to viscoelastic substrate subjected to antiplane shear. International Journal of Solids and Structures 36, 1781–1797.

Cook, T.S., Erdogan, F., 1972. Stresses in bonded materials with a crack perpendicular to the interface. International Journal of Engineering Science 10, 677–697.

Delale, F., Erdogan, F., 1981. Viscoelastic analysis of adhesively bonded joints. ASME Journal of Applied Mechanics 48, 331–338.

Erdogan, F., Aksogan, O., 1974. Bonded half planes containing an arbitrarily oriented crack. International Journal of Solids and Structures 10, 569–585.

Erdogan, F., Gupta, G.D., Cook, T.S., 1973. Numerical solution of singular integral equations. In: Sih, G.C. (Ed.), Mechanics of Fracture, vol. 1. Noordhoff, Groningen, pp. 368–425.

Goree, J.G., Venezia, W.A., 1977. Bonded elastic half-planes with an interface crack and a perpendicular intersecting crack that extends into the adjacent material. International Journal of Engineering Science 15, 1–17.

He, M.Y., Hutchinson, J.W., 1989. Crack deflection at an interface between dissimilar elastic materials. International Journal of Solids and Structures 25, 1053–1067.

Isida, M., Noguchi, H., 1993. Arbitrarily array of cracks in bonded half planes subjected to various loadings. Engineering Fracture Mechanics 46, 365–380.

Lee, E.H., 1962, Viscoelasticity. In: Flugge, W. (Ed.), Handbook of Engineering Mechanics. McGraw-Hill, New York, pp. 53–1 (Chapter 13).

Lu, H., Lardner, T.J., 1992. Mechanics of subinterface cracks in layered material. International Journal of Solids and Structures 29, 669–688.

Muskhelishvili, N.I., 1953. Some Basic Problems of the Mathematical Theory of Elasticity. Noordhoff, Groningen, The Netherlands.

Schapery, R.A., 1967. Stress analysis of viscoelastic composite materials. Journal of Composite Materials 1, 228–267.

Sills, L.B., Benveniste, Y., 1981. Steady state propagation of a mode III interface crack between dissimilar viscoelastic media. International Journal of Engineering Science 19, 1255–1268.

Sills, L.B., Benveniste, Y., 1983. Steady interface crack propagation between two viscoelastic standard solids. International Journal of Fracture 21, 243–260.

Suo, Z., 1989. Singularities interacting with interfaces and cracks. International Journal of Solids and Structures 25, 1133–1142.